Laboratory Demonstration of High Contrast with the PIAACMC Coronagraph on an Obstructed and Segmented Aperture

Ruslan Belikov[1], Dan Sirbu[1], David Marx[2], Camilo Mejia Prada[2], Eduardo Bendek[2], Eugene Pluzhnik[1], Stephen Bryson[1], Brian Kern[2], Olivier Guyon[3], Kevin Fogarty[1], Justin Knight[3], Dan Wilson[2], John Hagopian[5]

[1]NASA Ames Research Center, Moffett Field, CA, USA 94040;
[2]NASA Jet Propulsion Lab, Pasadena, CA, USA 91109;
[3]The University of Arizona, Tucson, AZ, USA 85719;
[4]Subaru Telescope (NAOJ), Hilo, HI, USA 96720;
[5]Lambda Consulting, Harwood, MD, USA 20776

ABSTRACT

Coronagraphs are an important technology to directly image and characterize exoplanets. Their efficiency has steadily been improving over the past several decades, but has not yet reached fundamental limits. In particular, the expected exoplanet yield for missions such as the Astro2020-recommended "IR/O/UV Flagship" can still be improved by factors of at least 2-4. One possible architecture that can enable at least a part of this improvement is the Phase-Induced Amplitude Apodization Complex Mask Coronagraph (PIAACMC). It features high throughput, small inner working angle (IWA), and almost no loss in PSF sharpness, and natively supports obstructed and segmented apertures. Historically, key disadvantages of PIAA have been poor tolerance to stellar angular sizes and maturity, but latest designs and demonstrations have made significant strides in this respect. We present the current status of our program to mature the PIAACMC technology. We first present our PIAACMC designs for LUVOIR-A and B, which resulted in improved expected yield of Exo-Earths relative to the baselines for both mission concepts. In particular, for LUVOIR-B, the yield improves from 28 to 42 due to improved tolerance to stellar angular size in our design. Our and vacuum demonstrations for the LUVOIR-A aperture at JPL's High Contrast Imaging Testbed (HCIT) include: 1.9e-8 raw contrast in 10% broadband light between 3.5 and 8 l/D; 4.1e-8 and 1.6e-9 coherent contrasts in monochromatic light between 2-4 and 4-8 l/D, respectively. We also present measurements and analysis of sensitivity to tip/tilt jitter and stellar angular size and compare our test results to models.

Keywords: coronagraph, high contrast, LUVOIR, exoplanet, direct imaging, PIAA, PIAACMC, habitable

1. OVERVIEW AND MOTIVATION FOR PIAA

Direct imaging of planets, and especially Earth-like planets, is an important goal of exoplanet science, and is one of the top recommendations of the Astro2020 decadal survey [1]. Although a direct image of an Earth-like planet around the nearest stars can in theory be accomplished with very small monolithic apertures as small as 0.45cm [2], much larger segmented mirrors are needed to do a survey for potentially habitable planets around dozens or hundreds of nearby stars. NASA's flagship studies LUVOIR [3] and HabEx [4] describe point designs to conduct such a survey. The LUVOIR concept has two options: LUVOIR A is based on a 15m on-axis segmented aperture with a central obstruction and spiders (Figure 1, left); and LUVOIR B is based on an 8m off-axis segmented aperture (Figure 1, right). In addition, the HabEx mission evaluated several segmented aperture options, but baselined a monolithic aperture, in part due to the perceived challenges of high performance coronagraphs on segmented apertures.

Astro2020 suggested a 6m off-axis telescope, but it is important to note that both the size, and whether the telescope is on-axis or off-axis, are still subject to trade. In particular, the motivation for an off-axis architecture has mostly to do with the fact that current coronagraph designs for off-axis apertures perform better than for on-axis apertures. However, this performance gap is not due to fundamental physics [5]. In other words, with sufficient engineering, coronagraphs on on-axis apertures should have comparable performance to off-axis apertures. More generally, physics-limited coronagraph performance is only weakly dependent on telescope aperture shape. On-axis apertures have significant advantages for

Space Telescopes and Instrumentation 2022: Optical, Infrared, and Millimeter Wave, edited by Laura E. Coyle, Shuji Matsuura, Marshall D. Perrin, Proc. of SPIE Vol. 12180, 1218025 · © 2022 SPIE · 0277-786X · doi: 10.1117/12.2630474

flagships: they are mechanically simpler, less risky, and are lower cost; they require smaller and lower cost sun-shields; and allow larger apertures for the same mass, volume, and/or price.

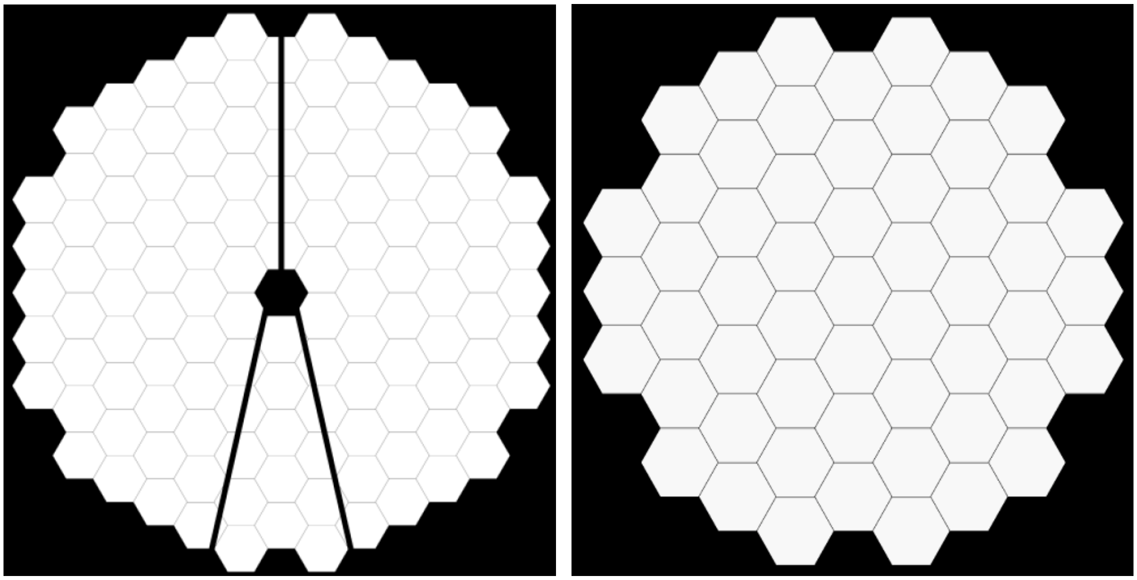

Figure 1.Left: LUVOIR A aperture (15m circumscribed diameter). Right: LUVOIR B aperture (8m circumscribed diameter). This paper primarily describes tests for the (more challenging) LUVOIR A aperture.

Furthermore, a key theme running through Astro2020 as well as several other studies of flagship missions [6,7] is that better and more thorough early trades and technology development are needed to lower the risk and cost of flagship missions. A good way of achieving this is more efficient and/or robust coronagraphic instruments. In theory, the Earth-like exoplanet yield of coronagraphs on a flagship mission can be improved by a factor of ~2-4 for off-axis and on-axis designs, respectively, simply by improving coronagraph efficiency and robustness to instabilities, for a given spectral band and quantum efficiency [5] (and even more if spectral band and QE can be improved). Such improvements in performance reduce many key risks and costs: the risk of $\eta_{\oplus}$ being low, the risk and cost associated with building an ultra-stable telescope, and the cost of a larger aperture. (Yield goes roughly as 2nd or 3rd power of telescope diameter [8], so that a factor of 4 improvement in yield can be equivalent to doubling the telescope aperture.)

It is not clear what coronagraph technologies can best improve the current state of the art and bring us closer to physics-limited performance, but the Phase Induced Amplitude Apodization (PIAA, [9]) family of coronagraphs is one promising path. PIAA achieves high level of starlight suppression by using two aspheric mirrors to apodize the pupil of the telescope. For the case of the "classical" PIAA coronagraph, this apodization suppresses the Airy diffraction rings of a stellar point spread function, revealing the star's planetary system. Classic PIAA provides high performance coronagraph designs for monolithic apertures, and a variant of PIAA called PIAACMC (PIAA Complex-valued Mask Coronagraph [10,11]) allows high performance on obstructed (and more generally, arbitrarily shaped) apertures. Similarly to PIAA, PIAACMC includes two aspheric mirrors which apodize the pupil. However, in addition to these two mirrors, PIAACMC also employs a partially transmissive pi-phase shifting mask. In practice, such an "ideal" mask is usually implemented by a fully reflective holographic mask, which emulates the far-field response of the ideal CMC mask. In theory, the PIAACMC coronagraph with an ideal CMC mask and no manufacturing errors is capable of fully suppressing an on-axis point source for any arbitrary aperture in broadband light. (Practical implementations of the CMC mask may never reach this ideal, but with sufficient engineering, they can come arbitrarily close.)

However, a key practical challenge for coronagraphs is sensitivity to stellar angular sizes, or equivalently, tip-tilt jitter of the telescope. For the case of the LUVOIR telescope, for example, some of the target stars have angular diameters on the order of 0.1 λ/D. Thus, a coronagraph design for such a telescope needs to suppress starlight for the case that a star is a disk (of mutually incoherent light) with ~0.1 λ/D diameter. In theory, there is a fundamental trade-off between inner working angle and sensitivity to stellar angular size, which applies not just to PIAA, but to all coronagraphs as a whole

[5]. In particular, coronagraphs with inner working angles of ~ 1 λ/D or less will not be able to achieve good stellar suppression in the presence of stars with 0.1 λ/D angular diameters. Fortunately, relaxing the inner working angle to 2 or 3 λ/D allows very deep suppression of such stars, although finding a design that achieves this for a particular coronagraph architecture can still be challenging.

For the case of monolithic apertures, the sensitivity to stellar angular size steadily improves as the inner working angle gets larger, both for PIAA and PIAACMC [10]. Therefore, coronagraph designs can readily be found for any desired stellar angular size, at the expense of the inner working angle. In addition, coronagraphs on segmented apertures (such as LUVOIR B) appear to perform similarly to monolithic apertures, because modern wavefront control systems appear to be able to mitigate the effects of segmentation, for many coronagraph architectures.

For the case of obstructed apertures, PIAACMC sensitivity to stellar angular size does not steadily improve with inner working angle, and in fact sometimes degrades. Nevertheless our PIAACMC design for LUVOIR A is tolerant to at least ~0.01 λ/D stellar angular diameter and was described in detail in [12]. This design improves LUVOIR A baseline yield from 47 to 51, based on simulations with the Altruistic Yield Optimizer [6] that modeled several coronagraphic instruments on the flagship working in tandem, choosing different ones for different targets. To be more precise, the best combination of coronagraphs involving PIAACMC have yield of 51, while the best combinations that do not have 47. Although these improvements fall short of the factor of 2-4 theoretical potential, further improvements are possible since we have not yet exhausted the design space (In particular, one promising path is the hybrid PIAA-vortex coronagraph [13]). In addition, our design enables targets that are not otherwise accessible, such as stars that are farther away and/or more later type stars such as K-dwarfs. Finally, our PIAA design for LUVOIR B is tolerant to 0.1 λ/D stellar angular diameter, and improves yield from 28 to 42. However, this paper focuses on testing of our LUVOIR A design in order to advance coronagraphic performance for the more challenging case: obstructed apertures.

2. REVIEW OF MODELING, HARDWARE, AND TEST SETUP

Our prior publications provide detailed coverage of our PIAACMC design [12], modeling [14,15], as well as testing procedures and initial results [16], which we briefly review here.

The PIAACMC design we manufactured and tested is similar to the one for the mission with one key difference – we optimized the testbed design for a one-sided (180º) dark zone rather than the full double-sided (360º) one. This was done because it allowed for testing with one deformable mirror rather than two, which served to simplify the system and better isolate the key items we were testing for (contrast in the dark zone and robustness to low order aberrations, which are not strongly dependent on whether one or two DMs are used, according to models). This design achieves 4.83e-10 raw contrast in simulation between 2 and 8 l/D in a 10% band for a point sources, and stays below 1e-9 for up to 0.02 λ/D diameter stars, representing significantly improved tolerance to stellar diameter than prior PIAA designs. A combination of CMC mask and DM were tuned to provide high contrast for a dark zone between 2 and 8 l/D, but this PIAA mirror design allows IWAs as small as 1.4 λ/D (with a different CMC and DM shapes, though this would make it more sensitive to tip/tilt and stellar size). We have not fully explored the trade space of this architecture and in particular, designs with contrasts < 1e-10 are possible (with a less aggressive inner working angle or tolerance to aberrations), but we settled on this design as having a good combination of performance parameters for testing at HCIT.

Our tests were conducted at the High Contrast Imaging Testbed (HCIT) facility at NASA JPL, but due to the fact that PIAA layout is not readily compatible with existing HCIT testbeds such as DST, we created an entirely new testbed for our project, shown schematically in Figure 2. Key components of the layout are as follows. First, a single mode fiber and a pinhole serve as a point source of light representing a star, with monochromatic as well as broadband laser options available. This light is then relayed to a pupil mask representing the LUVOIR A pupil (manufactured by Lambda Consulting using carbon nanotube technology). Light is next relayed to a PIAA system (by NuTek), consisting of a tube with two PIAA mirrors with a hole in the middle corresponding to the pupil obstruction, allowing entry and exit of the light beam. A Boston Micromachines Corporation Kilo-DM with 952 actuators is conjugated to the downstream PIAA mirror (PIAA2) and performs wavefront control. Finally, a CMC mask (by NASA JPL MDL), Lyot tsop (by Lambda Consulting), and field stop complete the coronagraphic setup. The final camera can move along the z-axis, covering the range from focus to pupil-conjugate. A polarizer (analyzer) was also placed in front of the camera to isolate polarization effects from other limiting factors, although we have not performed detailed tests of whether polarization was a concern in our system.

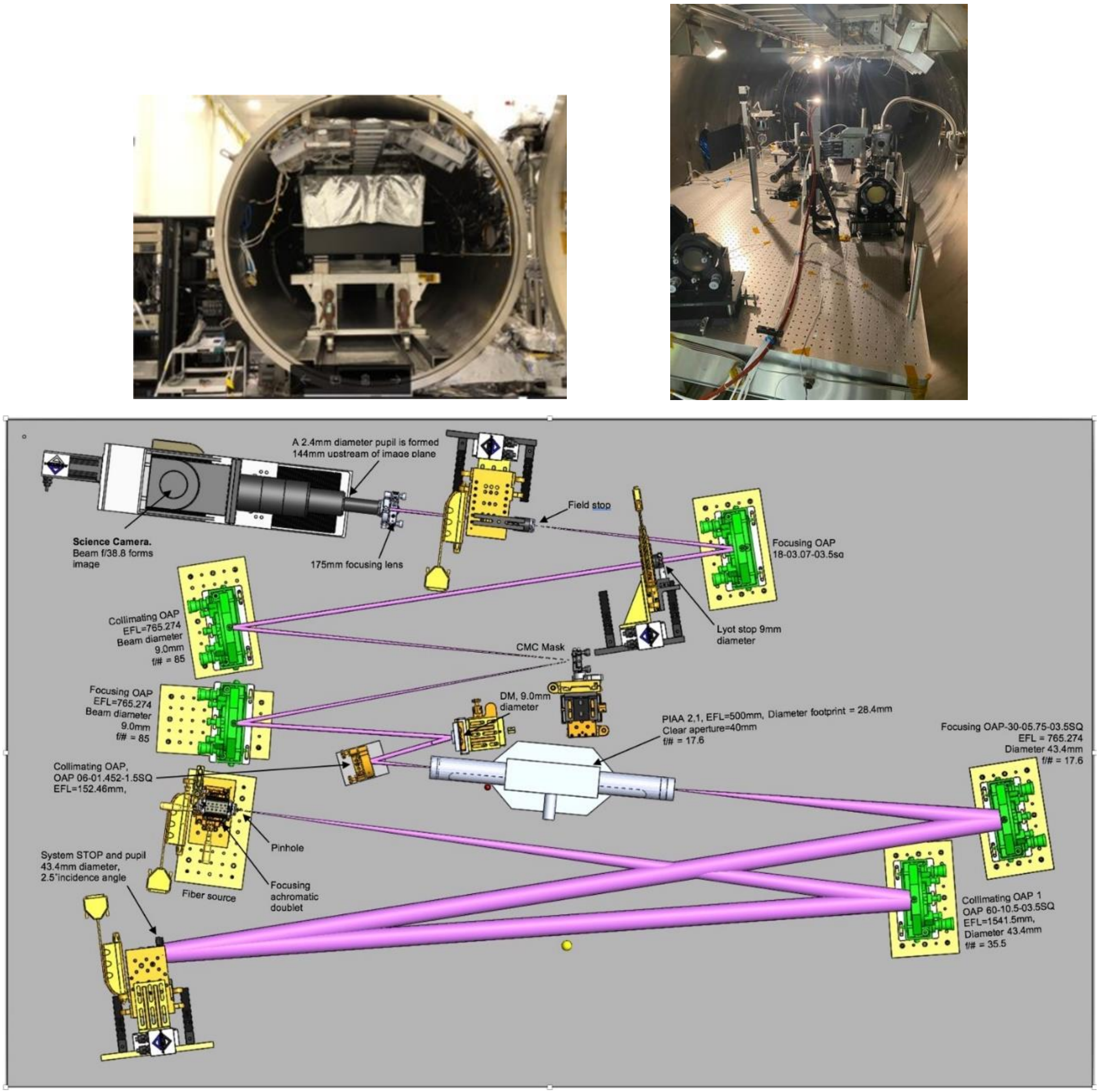

Figure 2. Top: One of the vacuum chambers in the High Contrast Imaging Testbed chamber (HCIT) at NASA JPL (left) and PIAACMC bench (right). Bottom: Test layout of the PIAACMC coronagraph used for the results in this paper.

Initially, we observed significant mismatches between our model and testbed measurements, but after several iterations of hardware and modeling, we are now achieving a good match [14]. In particular, empirically measured pupil plane and focal plane illumination match, with and without the CMC mask, to within about 10% over the majority of the illuminated region. In addition, our model calibrations relied not only on measurements of the intensities of different planes in different hardware configurations, but also a phase retrieval procedure to estimate the wavefront error in the system (which separately estimated low order errors upstream and downstream of PIAA). Finally, plate scale as well as DM scale and registration were all empirically calibrated and folded into our models of the system and wavefront control algorithms. Our main wavefront control algorithm was standard pair-wise Electric Field Conjugation (EFC, [17]), although we also used our project as an opportunity to try several other techniques (outside the scope of this paper), including classical speckle nulling and experimental self-calibrating control methods.

Contrasts for monochromatic light (λ_0 = 675nm); dark zone: 4-8 λ/D

9.0e-9 | 1.6e-9 | 7.4e-9 | 1D azimuthal average

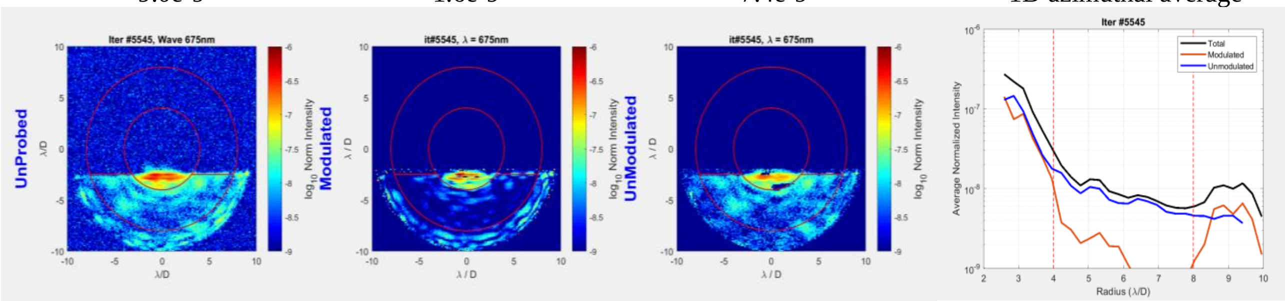

Contrasts for monochromatic light (λ_0 = 675nm); dark zone: 2-4 λ/D

1.1e-7 | 4.1e-8 | 7.0e-8 | 1D azimuthal average

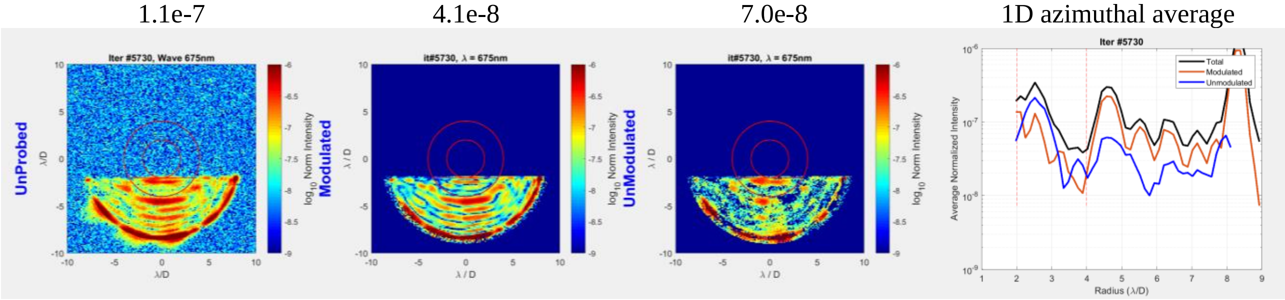

Contrasts for 2% broadband light (λ_0 = 650nm); dark zone: 3.5-8 λ/D

1.1e-8 | 1.8e-9 | 8.9e-9 | 1D azimuthal average

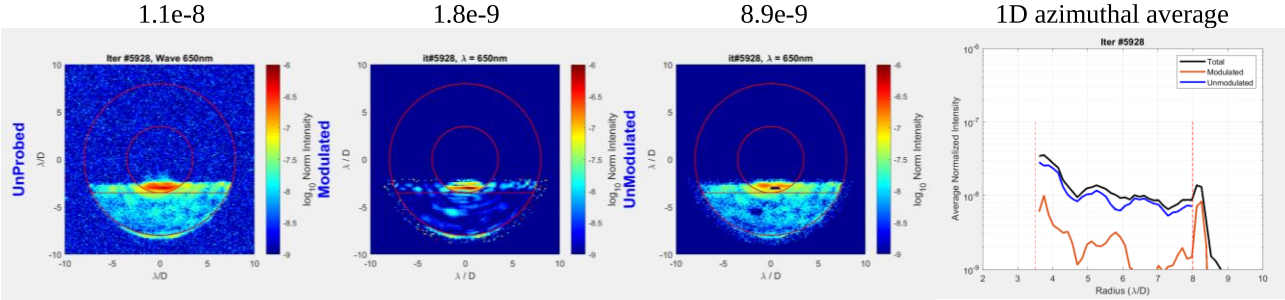

Contrasts for 10% broadband light (λ_0 = 650nm); dark zone: 3.5-8 λ/D

1.9e-8 | 9.4e-9 | 9.4e-9 | 1D azimuthal average

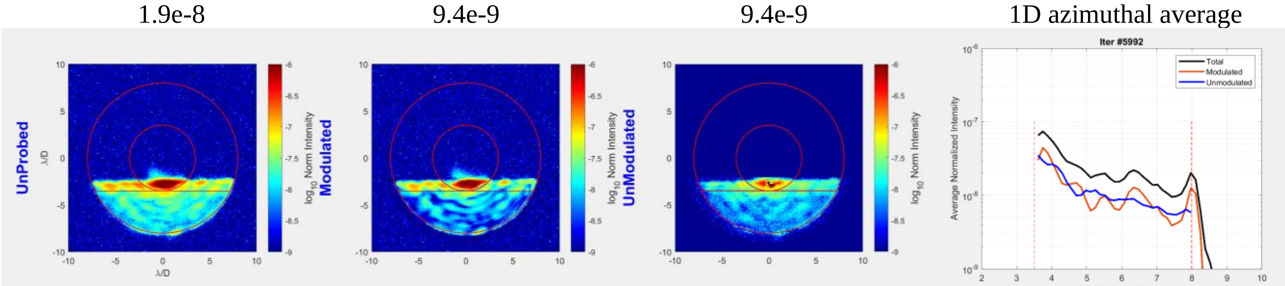

Figure 3. Laboratory results. Rows correspond to different wavelength bands and dark zones (indicated by red outlines). Columns represent, respectively, raw (unprobed), coherent (modulated), and incoherent (unmodulated) images, and 1D azimuthal averages. A D-shaped field stop was used to prevent blooming of surrounding bright speckles.

3. LABORATORY CONTRAST MEASUREMENTS

We performed tests to create high contrast dark zones with EFC under several different conditions (see Figure 3), including monochromatic light with a diode laser (675nm) as well as broadband light (centered on 650nm) in a 2% and 10% band, and different sized dark zones. Figure 3 presents the dark zones after EFC converged in each case, showing the raw dark-subtracted images in the leftmost column ("unprobed"). These images consists of coherent and incoherent components shown in columns 2 and 3. (These are also referred to as "modulated" and "unmodulated", meaning a component that is susceptible to modulation by the DM, and a component that is not.) The rightmost column shows 1D azimuthal averages of all three images. The images show light in a D-shape region that is admitted by the field stop (with some light diffracting outside the physical edges of the field stop), and the dark zone radii are shown as red circles. Typically, the dark zone is smaller than the field stop, and the EFC control region is slightly larger than the actual dark zone. Contrast values shown in the figure are averages across the dark zone.

Our monochromatic tests (first two rows in Figure 3) were done separately in the 2-4 and 4-8 λ/D regions. This was because we observed a bright speckle at the inner edge of the field stop which proved challenging to remove, and limited our contrast to 1.1e-7 (4.1e-8 modulated) in the 2-4 region. The nature of this speckle remains under investigation, and in particular whether or not it has to do with coronagraph hardware or testbed itself. This speckle was originally thought to be due to testbed jitter and tip/tilt sensitivity, but this has been ruled out. Another possibility is diffraction from the field stop edge. The field stop is not a fundamentally required component of a coronagraph and is present to prevent practical issues such as camera blooming and other pixel cross-talk. (In which case a camera with less blooming and cross-talk would mitigate this.)

Contrast in the 4-8 region was much deeper, at 9e-9 raw (1.6e-9 modulated), proving that PIAACMC components impose no incoherent light limits down to at least 1.6e-9 levels. The unmodulated light is at 7.4e-9 levels and is what is ultimately limiting our performance. It is not yet known whether this light is due to PIAACMC components or auxiliary testbed hardware and environment. However, this unmodulated light was originally much higher, which was traced to several effects external to the PIAACMC coronagraph, such as ghosts and scattered light, and this may still be what's limiting both the raw and modulated contrast.

Performance in the 2% band is only marginally worse than the monochromatic light 4-8 λ/D case, and may in fact represent better performance considering that wavefront control was applied over a larger dark zone (3.5-8 λ/D). We conclude that our system is insensitive to increasing the band to 2%, and that we do not have ghosts whose optical path difference is between the coherence length of the monochromatic diode and 2% band source.

Finally, raw contrast performance in a 10% band is 1.9e-8 in 10% between 3.5-8 λ/D, which is comparable (within roughly a factor of 2) of monochromatic and 2% cases. Furthermore, levels of unmodulated light are similar. The greatest difference is the unmodulated light, which at 9.4e-9 is almost an order of magnitude greater than the narrowband case. Analysis of different wavelengths in the 10% band reveals a quadratic dependence of contrast vs. wavelength, with the contrast at the central wavelength being much closer to the narrowband case. Therefore, unlike the monochromatic case, broadband contrast appears to be limited by the chromaticity in our system, rather than incoherent light. However, according to simulations of broadband EFC, this chromaticity should be suppressible, and it may be the case that we have simply not spent enough time on tuning our broadband models (we focused on monochromatic and narrowband tests as a prerequisite for broadband).

4. TIP-TILT SENSITIVITY MEASUREMENTS

One of the historical weaknesses of PIAA family of coronagraphs is its sensitivity to tip/tilt aberrations (and by extension, to stellar angular size). Our LUVOIR A was designed with improved tolerance to tip/tilt aberrations and according to models is insensitive to ~0.02 λ/D diameter stars down to ~1e-9 contrast. However, does actual tolerance match the design?

To test this, we moved our source off axis by small amounts and collected the resulting coronagraphic off-axis PSFs. Raw contrast measurements both in the model and testbed are shown in Figure 4 (top), for the full 2-8 λ/D dark zone. On this figure, solid thin lines show the model, and dashed lines show the measurement. The "x" and "y" coordinates correspond to the orientation shown in Figure 3 (in other words, "x" corresponds to motion of the source parallel to the straight edge of the dark zone, and "y" is perpendicular – as might be expected, sensitivity is greater in "y" than in "x", which is consistent with Figure 3). However, all of these curves mix modes that are insensitive to tip/tilt (due to the underlying speckle field), and terms that are sensitive to tip/tilt (which is what we really want to compare). The former is responsible for the horizontal parts of the curves, which are greater for the empirical case due to the contrast limitations described in section 3. This mixing of modes makes the comparison non-trivial if the underlying speckle fields are significantly different between empirical measurements and model, as they are in Figure 4. However, it is possible to disentangle the pure tip/tilt terms. The details of how this is done is beyond the scope of this paper (and will be covered in a journal paper), but our empirical estimates of pure tip/tilt terms are shown as solid lines, which compare well to the slanted portions of the design curves where the tip/tilt terms dominate. We conclude that the observed sensitivity to tip/tilt aberrations compares well to the designed one.

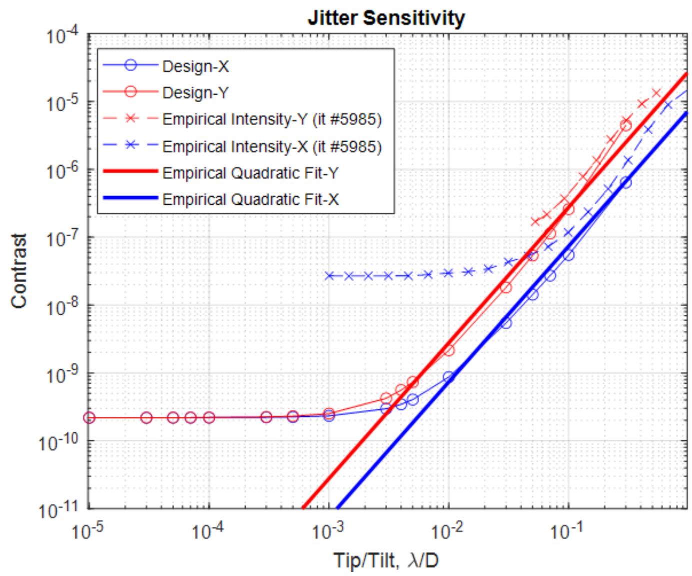

Figure 4. Top: Comparison of tip/tilt sensitivities between model and testbed.

5. PRELIMINARY ANALYSIS OF LIMITING FACTORS

A full analysis of limiting factors is ongoing and is outside the scope of this paper, but we present a few preliminary findings here. First, it is important to note that, generally speaking, the majority of a dozen or more limiting factors we encountered on the path to current performance in Figure 3 were not due to any kind of fundamental limitation of the PIAACMC technology, but rather the development of the testbed itself. It is not known yet whether the current limits are due to some kind of fundamental limitation of PIAACMC, but we have certainly not exhausted testbed and model improvements, especially in broadband light. It is therefore quite possible that, had the project gone on for longer, performance could be further improved to ~1e-9 raw contrast levels predicted by models.

A key limiting factor we were able to rule out is sensitivity to tip/tilt aberrations. Measured jitter levels on the testbed are about 0.01 λ/D rms in x and 0.0034 λ/D in y. From Figure 4, this should result in unmodulated contrast on the order of 1e-9, well below the levels we actually observe, especially in the 2-4 λ/D dark zone. However, it is still possible that the source is not truly single mode and is acting as a star with a diameter that is too large. Another potential limiting factor is manufacturing and alignment errors. When we fold in all known errors into our models, our contrast performance stays below 1e-9 in 10% between 2 and 8 λ/D, but there may be unknown terms on the testbed that cause limits before 1e-9.

Other limiting factors we ruled out, or determined are not likely are: voltage resolution on the deformable mirror, most types of ghosts, chromaticity due to Fresnel diffraction, and out-of-band light present in our source. Limiting factors under investigation that are PIAACMC-related include sub-wavelength electric field interactions on the CMC mask, and polarization effects (that are not isolated by our polarizer). Ones that are not PIAACMC-related include sub-wavelength electric field interactions with the carbon nanotube pupil mask, the pinhole, DM jitter, certain types of ghosts, and insufficient software parameter tuning.

6. CONCLUSIONS

There is a significant gap between current coronagraph performance and theoretical limits, especially for obstructed apertures, which remain important because they represent a path for significant risk and cost savings on the Astro2020 mission, assuming the performance gap between coronagraphs on on-axis and off-axis apertures can be closed. PIAACMC technology is one path that may bridge both gaps, at least partially. Our PIAACMC and PIAA designs for LUVOIR show improved performance over baselined designs, especially for LUVOIR B, where the improvement in yield of characterized exoEarths is from 28 to 42. For LUVOIR A, the improvement is more modest (47 to 51), but allows new targets that are not otherwise possible. Furthermore, further improvements may be possible for obstructed apertures such as LUVOIR A, especially with the new PIAA-vortex concept.

Our current performance in the lab includes 9e-9 raw contrast (1.6e-9 coherent) for a 4-8 λ/D dark zone in monochromatic light; 1.1e-7 raw (4.1e-8 coherent) for 2-4 l/D in monochromatic light; and 1.9e-8 (9.4e-9 coherent) in 10% broadband light. In addition, both our design, and our empirical measurements, show tolerance to 0.02 λ/D diameter stars down to ~1e-9. Further improvements may be possible for PIAACMC, and are known to be possible for PIAA-vortex variant.

A full analysis of limiting factors is under way, but we have ruled out tip/tilt sensitivity, and a number of others, such as sensitivities to known errors, voltage resolution on the deformable mirror, most types of ghosts, chromaticity due to Fresnel diffraction, and out-of-band light present in our source. Most of our prior limiting factors have been related to the development of a new testbed for PIAACMC, rather than PIAACMC itself. Although it remains possible that our limiting factor is due to some unknown fundamental limitation of the PIAACMC architecture or hardware, we have not yet exhausted possible testbed and software improvements that could have led to better performance before the testing phase of this project concluded.

7. ACKNOWLEDGEMENTS

This work was supported in part by the National Aeronautics and Space Administration's Ames Research Center, as well as the NASA Strategic Astrophysics Technology – Technology Development for Exoplanet Missions (SAT-TDEM) program through solicitation NNH16ZDA001N-SAT at NASA's Science Mission Directorate. It was carried out at the NASA Ames Research Center, the NASA Jet Propulsion Laboratory, and the University of Arizona. Any opinions, findings, and conclusions or recommendations expressed in this article are those of the authors and do not necessarily reflect the views of the National Aeronautics and Space Administration.

REFERENCES

[1] National Academies of Sciences, Engineering, and Medicine 2021. *Pathways to Discovery in Astronomy and Astrophysics for the 2020s*. Washington, DC: The National Academies Press. https://doi.org/10.17226/26141.

[2] Belikov, R., Bendek, E. A., Thomas, S., J., Males, J. R., Lozi, J., "How to directly image a habitable planet around Alpha Centauri with a ~30-45cm space telescope," *Proc SPIE* 9605-41, (2015).

[3] B. S. Gaudi, S. Seager, B. Mennesson, A. Kiessling, K. Warfield, G. Kuan, K. Cahoy, J. T. Clarke, S. Domagal-Goldman, L. Feinberg, O. Guyon, J. Kasdin, D. Mawet, T. Robinson, L. Rogers, P. Scowen, R. Somerville, K. Stapelfeldt, C. Stark, D. Stern, M. Turnbull, S. Martin, O. Alvarez-Salazar, R. Amini, W. Arnold, B. Balasubramanian, M. Baysinger, L. Blais, T. Brooks, R. Calvet, V. Cormarkovic, C. Cox, R. Danner, J. Davis, L. Dorsett, M. Effinger, R. Eng, J. Garcia, J. Gaskin, J. Harris, S. Howe, B. Knight, J. Krist, D. Levine, M. Li, D. Lisman, M. Mandic, L. Marchen, C. Marrese-Reading, J. McGowen, A. Miyaguchi, R. Morgan, B. Nemati, S. Nikzad, J. Nissen, M. Novicki, T. Perrine, D. Redding, M. Richards, M. Rud, D. Scharf, G. Serabyn, S. Shaklan, S. Smith, M. Stahl, P. Stahl, H. Tang, D. Van Buren, J. Villal-vazo, S.Warwick, D.Webb, R.Wofford, J.Woo, M.Wood, J. Ziemer, E. Douglas, V. Faramaz, S. Hildebrandt, T. Meshkat, P. Plavchan, G. Ruane, and N. Turner, Habitable Exoplanet Observatory Final Report," tech. rep., Jet Propulsion Laboratory, August 2019.

[4] D. Fischer, B. Peterson, J. Bean, D. Calzetti, R. Dawson, C. Dressing, L. Feinberg, K. France, O. Guyon, W. Harris, M. Marley, V. Meadows, L. Moustakas, J. O'meara, I. Pascucci, M. Postman, L. Pueyo, D. Redding, J. Rigby, A. Roberge, D. Schiminovich, B. Schmidt, K. Stapelfeldt, C. Stark, and J. Tumlinson, LUVOIR Final Report," tech. rep., NASA, 2019.

[5] Belikov, R., Sirbu, D., Jewell, J., Guyon, O., Stark, C, “Theoretical performance limits for coronagraphs on obstructed and unobstructed apertures: how much can current designs be improved?,” *Proc SPIE 11823* (2021).

[6] https://science.nasa.gov/about-us/large-mission-study

[7] R. E. Bitten, S. A. Shinn and D. L. Emmons, "Challenges and Potential Solutions to Develop and Fund NASA Flagship Missions," 2019 *IEEE Aerospace Conference*, 2019, pp. 1-13, doi: 10.1109/AERO.2019.8741920.Belikov, R., Sirbu, D., Jewell, J., Guyon, O., Stark, C, “Theoretical performance limits for coronagraphs on obstructed and unobstructed apertures: how much can current designs be improved?,” Proc SPIE 11823 (2021).

[8] Stark, C. C., Belikov, R., Bolcar, M. R., Cady, E., Crill, B.P., Ertel, S., Groff, T., Hildebrandt, S., Krist, J., Lisman, P.D., Mazoyer, J., Mennesson, B., Menati, B., Pueyo, L., Rauscher, B.J., Riggs, A.J., Ruane, G., Shaklan, S.B., Sirbu, D., Soummer, R., St. Laurent, K., Zimmerman, N., “The ExoEarth Yield Landscape for Future Direct Imaging Space Telescopes,” *accepted by JATIS*, (2019).

[9] Guyon, O., “"Phase-induced amplitude apodization of telescope pupils for extrasolar terrestrial planet imaging," *A&A*, v.404, p. 379-387 (2003).

[10] Guyon, O., Martinache, F., Belikov, R., Soummer, R., "High performance PIAA coronagraphy with complex amplitude focal plane masks," *ApJS 190,* 2, pp. 220-232 (2010).

[11] Guyon, O., Hinz, P.M., Cady, E., Belikov, R., Martinache, F. 2014, “High Performance Lyot and PIAA Coronagraphy for Arbitrarily Shaped Telescope Apertures,” *ApJ* **780**, 171.

[12] Belikov, R., Bryson, S., Sirbu, D., Guyon, O., Bendek, E., Kern, B., “Design and performance analysis of a PIAACMC coronagraph on a segmented aperture,” Proc SPIE 10698 (2018).

[13] Fogarty, K., Sirbu, D., Belikov, R., Pluzhnik, E., “The PIAA-Vortex Coronagraph: a New Coronagraph Technology to Maximize Exo-Earth Yields in the Astro2020 Era,”, *Proc of SPIE* 12180 (2022).

[14] Sirbu, D., Marx, D., Belikov, R., Bendek, E., Fogarty, K., Kern, B., Guyon, O., Pluzhnyk, E., Wilson, D., “Model validation of phase-induced amplitude apodization complex mask coronagraph for LUVOIR-A in vacuum,” Proc SPIE 11823 (2021).

[15] Newman, K., Belikov, R., Guyon, O., “Performance characterization of a phase-induced amplitude apodization complex focal plane mask,” *Proc SPIE 10563* (2017).

[16] Marx, D., Belikov, R., Sirbu, D., Kern, B., Prada, C., Bendek, E., Wilson, D., “Results from the laboratory demonstration of a PIAACMC coronagraph with a segmented aperture,” Proc SPIE 11823 (2021).

[17] Give’on, A., Kern, B. K., and Shaklan, S., “Pair-wise, deformable mirror, image plane-based diversity electric field estimation for high contrast coronagraphy,” Proc. SPIE 8151, 815110-01-10 (2011).